Simulation of MPPT Algorithm for a Grid-Connected Photovoltaic Power System

Davu swetha
M.Tech student , Sri chaitanya college of engineering

T.Rajani(Associate professor)
Sri chaitanya college of engineering

Abstract:- A photovoltaic (PV) power system which is connected to grid with high voltage gain is proposed, and the steady-state model analysis and the control strategy of the system are presented in this paper. For a typical PV array, the output voltage is relatively low, and a high voltage gain is obligatory to realize the grid-connected function. The proposed PV system employs a ZVT-interleaved boost converter with winding-coupled inductors and active-clamp circuits as the one power-processing stage, which can boost a low voltage of the PV array up to a high dc-bus voltage. Accordingly, an accurate steady-state model is obtained and verified by the simulation and experimental results, and a transformer less inverter with bidirectional power flow is used as the another power-processing stage, which can stabilize the dc-bus voltage .If transformer is removed the galvanic isolation between the pv generator and the grid is lost, this may cause safety hazards in the event of ground faults. Two compensation units are added to perform in the system control loops to achieve the low total harmonic distortion and fast dynamic response of the output current. Furthermore, a simple maximum-power-point-tracking method based on power balance is applied in the PV system to reduce the system complexity

Index Terms— **Bidirectional power flow control, compensation units, direct current control, maximum-power-point-tracking (MPPT) method, photovoltaic (PV) system, steady-state model**

I.   INTRODUCTION

Today photovoltaic (PV) power systems are becoming more and more popular, with the increase of energy demand and the concern of environmental pollution around the world. Four different system configurations are widely developed in grid-connected PV power applications: the centralized inverter system, the string inverter system, the multi string inverter system and the module-integrated inverter system [1]–[4]. Generally three types of inverter systems except the centralized inverter system can be employed as small-scale distributed generation (DG) systems, such as residential power applications. The most important design constraint of the PV DG system is to obtain a high voltage gain. For a typical PV module, the open-circuit voltage is about 21 V and the maximum power point (MPP) voltage is about 16 V. And the utility grid voltage is 220 or 110Vac. Therefore, the high voltage amplification is obligatory to realize the grid-connected function and achieve the low total harmonic distortion (THD). The conventional system requires large numbers of PV modules in series, and the normal PV array voltage is between 150 and 450 V, and the system power is more than 500 W. This system is not applicable to the module-integrated inverters, because the typical power rating of the module-integrated inverter system is below 500 W [3], [4], and the modules with power ratings between 100 and 200 W are also quite common [5]. The other method is to use a line frequency step-up transformer, and the normal PV array voltage is between 30 and 150 V [3], [4]. But the line frequency transformer has the disadvantages of larger size and weight

In the grid-connected PV system, power electronic inverters are needed to realize the power conversion, grid interconnection, and control optimization [6], [7]. Generally, gird-connected pulsewidth modulation (PWM) voltage source inverters (VSIs) are widely applied in PV systems, which have two functions atleast because of the unique features of PV modules. First, the dc-bus voltage of the inverter should be stabilized to a specific value because the output voltage of the PV modules varies with temperature, irradiance, and the effect of maximum power-point tracking (MPPT). Second, the energy should be fed from the PV modules into the utility grid by inverting the dc current into a sinusoidal waveform synchronized with utility grid. Therefore, it is clear that for the inverter-based PV system, the conversion power quality including the low THD, high power factor, and fast dynamic response, largely depends on the control strategy adopted by the grid-connected inverters.

In this paper, a grid-connected PV power system with high voltage gain is proposed. The steady-state model analysis and the control strategy of the system are presented. The grid connected PV system includes two power-processing stages: a high step-up ZVT-interleaved boost converter for boosting a low voltage of PV array up to the high dc-bus voltage, which is not less than grid voltage level; and a full-bridge inverter for in verting the dc current into a sinusoidal waveform synchronized with the utility grid. Furthermore, the dc–dc converter is responsible for the MPPT and the dc–ac inverter has the capability of stabilizing the dc-bus voltage to a specific value.

The grid-connected PV power system can offer a high voltage gain and guarantee the used PV array voltage is less than 50 V, while the power system interfaces the utility grid. On the one hand, the required quantity of PV modules in series is greatly reduced. And the system power can be controlled in a wide range from several hundred to thousand watts only by changing the quantity of PV module branches in parallel. Therefore, the proposed system can not only be applied to the string or multi-string inverter system, but also to the module-integrated inverter

1

system in low power applications. On the other hand, the non-isolation PV systems employing neutral-point-clamped (NPC)
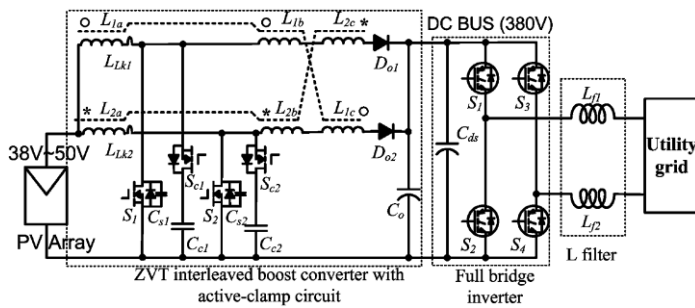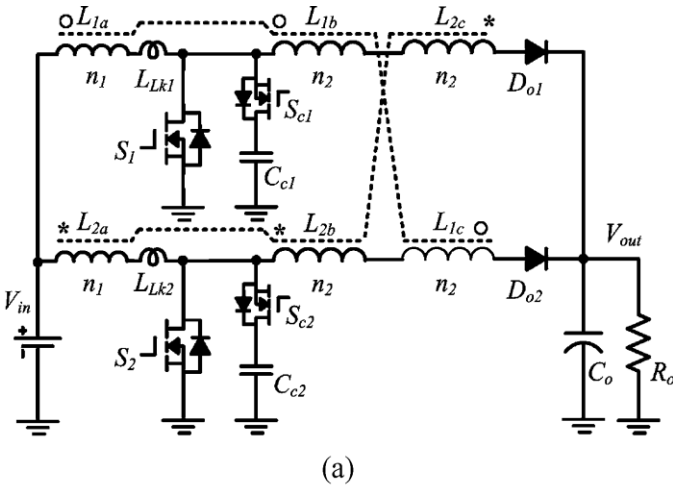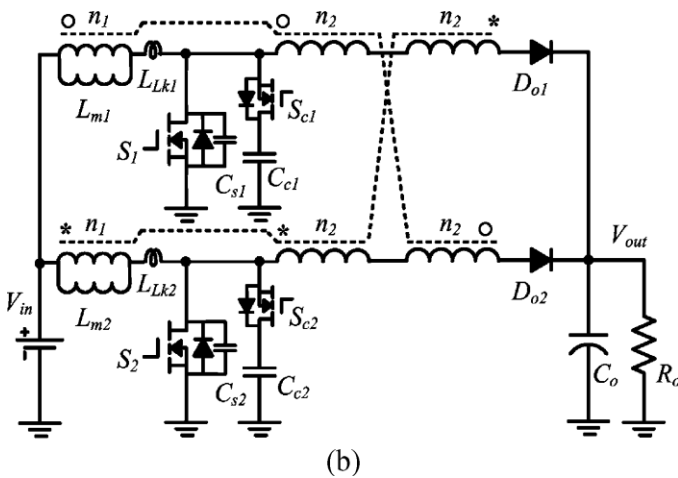

Fig. 1. Proposed grid-connected PV power system.

Fig. 2. High step-up ZVT-interleaved boost converter and its equivalent circuit. (a) ZVT-interleaved boost converter. (b) Equivalent circuit.

topology, highly efficient reliable inverter concept (HERIC) topology, H5 topology, etc. [8]–[14], have been widely used especially in Europe. Although the transformerless system having a floating and non earth-connected PV dc bus requires

more protection [10], [15], [16], it has several advantages such as high efficiency, lightweight, etc. Therefore, the non isolation scheme in this paper is quite applicable by employing the high step-upZVT-interleaved boost converter, because high voltage gain of the converter ensures that the PVarray voltage is below50Vand benefits the personal safety even if in high-power application.

II. STEADY-STATE MODEL OF HIGH STEP-UP ZVT-INTERLEAVED BOOST CONVERTER

Fig. 2 shows the ZVT-interleaved boost converter with winding-coupled inductors and active-clamp circuits, which is proposed by our research team [11]. The winding-coupled inductors offer the voltage-gain extension. The active-clamp circuits realize the ZVT commutation of the main switches and the auxiliary switches[11]

As shown in Fig. 2(a), S1 and S2 are the main switches; Sc1 and Sc2 are the active- clamp switches; Do1 and Do2 are the output diodes. The coupling method of the winding-coupled inductors is marked by open circles and asterisks. Each coupled inductor is modeled as the combination of a magnetizing inductor, an ideal transformer with corresponding turns ratio and a leakage inductor in series with the magnetizing inductor. The equivalent circuit model is demonstrated in Fig. 2(b), where Lm 1 and Lm 2 are the magnetizing inductors; Llk 1 and Llk 2 are the leakage inductors including the reflected leakage inductors of the second and third windings of the coupled inductors; Cs1 and Cs2 are the parallel capacitors, including the parasitic capacitors of the switches; Cc1 and Cc2 are the clamp capacitors; N is the turns ratio n2 /n1 .

Compared with the proposed converter, the full-bridge dc–dc converter is also employed commonly as a similar first stage in the PV system. However, for the high step-up gain applications, the large current ripples of the primary-side switches increase the conduction losses, and the secondary-side diodes need to sustain a high voltage stress. Moreover, as a buck- type converter, a large turns ratio of the transformer is necessary to obtain a high step-up gain, which induces a large leakage inductance and large commutation energy on the primary-side switches. Therefore, the design of the transformer is difficult and the converter's efficiency is impacted. Furthermore, the resonant-mode converters such as LLC, LCC, and higher order element converters are studied and developed, which are attractive for potential higher efficiency and higher power density than PWM counterparts. However, most of resonant converters include some inherent problems, such as electromagnetic interference (EMI) problems due to variable frequency operation and reduced conversion efficiency due to circulating energy generation. Moreover, to make practical use of the resonant converters, the required precise control waveform and difficult over current protection increase the design complexity of the whole system. Correspondingly the ZVT-interleaved boost converter has the following three main advantages.

(1) Voltage gain is extended greatly by using a proper turns ratio

2

design. As the turns ratio increases, the voltage gain increases without the extreme duty ratio, which can reduces the input and output current ripples. Omitting the effect of the leakage inductance and applying the voltage second balance to the

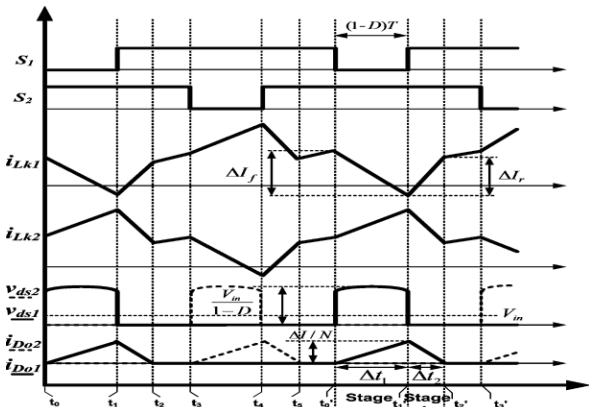$$M = \frac{V_{\text{out}}}{V_{\text{in}}} = \frac{N+1}{1-D}.$$

(2) Voltage stress of the main switches is reduced, as the turns ratio increases. Therefore, the low-voltage and high performance devices can be used to reduce the switching and conduction losses. And the voltage spikes are clamped effectively and the leakage energy is recovered. If the clamp capacitance is assumed large enough and the voltage ripple on the switches can be ignored when they turn

3) ZVT soft switching is achieved for both main switches and auxiliary switches during the whole switching transition, which means the switching losses are reduced greatly. Diode reverse-recovery loss is greatly reduced because the di/dt of the diode current is controlled by the inherent leakage inductor of a coupled boost inductor.

Unfortunately, the leakage inductor of the winding-coupled inductors has great effect on the voltage gain expression and a big error is found in the steady-state model based on (1), especially when the leakage inductance increases to a certain level, which brings difficulty to the design of circuit parameters. To derive a more accurate steady-state model of the converter, the leakage inductance of the winding-coupled inductors should be considered, since the leakage inductance strongly influences the operation states of the circuit. To simplify the calculation, the following conditions are assumed in reason.

(1) The clamp capacitance is large enough, so the voltage ripple on the main switches can be ignored and the voltage Vds is taken as a constant when they turn off.

2) The magnetizing inductance is much larger than the leakage inductance, so the magnetizing current IL m is taken as a constant in one switching period.

3) The dead times of the main switches and the corresponding auxiliary switches are ignored.

4) The two interleaved and inter coupled boost converter cells are provided with a strict symmetry.

Based on the previous assumptions, the partial key waveforms

this converter are shown in Fig. 3, which have reached a steadystate.

$$M = \frac{V_{\text{out}}}{V_{\text{in}}}$$
$$= (N+1)\frac{\sqrt{[(1-D)R]^2 + 8N^2 f_s L_{lk} R} - (1-D)R}{4N^2 \times f_s \times L_{lk}}$$

where Llk is the equivalent leakage inductance of the winding-coupled inductors, and Llk = Llk 1 = Llk 2 , and R is the equivalent load of the converter.

As shown in Table I, the results calculated by the two steady-state models and the simulation software PSIM, are compared to verify the proposed model. From the data in Table I, the maximum error of the output voltage between the accurate model based on (3) and the simulation results is only 0.6%, and the corresponding maximum error of the model based on (1) reaches up to 43.1%.

III. CONTROL STRATEGY OF FULL-BRIDGE INVERTER WITHBIDIRECTIONAL POWER FLOW

TABLE I
STEADY-STATE MODEL VERIFICATION

Parameters						
V_{in}		48V		f_s		50kHz
L_{m1}, L_{m2}		200 μH		R		100 Ω
C_{c1}, C_{c2}		2.2 μF		C_{s1}, C_{s2}:		2.2nF

| N	L_{lk} (μH)	D	PSIM Simulation V_{out}(V)	Model based on equation (1) V_{out}(V)	Error	Accurate model based on equation (21) V_{out}(V)	Error
2	4	0.65	368.4	411.4	11.7%	368.4	0%
3	4	0.65	442.4	548.6	24.0%	443.3	0.2%
2	5	0.65	359.0	411.4	14.6%	360.0	0.3%
3	5	0.65	424.5	548.6	29.2%	426.7	0.5%
2	6	0.65	350.4	411.4	17.4%	352.3	0.5%
3	6	0.65	408.9	548.6	34.2%	411.1	0.6%
2	4	0.7	416.6	480.0	15.2%	415.9	-0.2%
3	4	0.7	489.6	640.0	30.7%	490.0	0.1%
2	5	0.7	403.9	480.0	18.8%	402.3	-0.4%
3	5	0.7	468.5	640.0	36.6%	466.7	-0.4%
2	6	0.7	393.8	480.0	21.9%	392.3	-0.4%
3	6	0.7	447.2	640.0	43.1%	450.0	0.6%
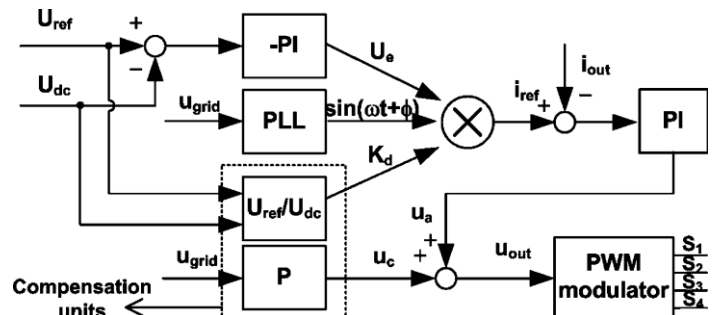
Fig.4 control block of full-bridge inverter with bidirectional power flow

power facilitates the compensation of the dc-bus and the ac-side voltage variations, which helps to stabilize the dc-bus voltage in startup and cloudy situations and improves the stability of overall system. Fig. 4 shows the control block of the full-bridge inverter with bidirectional power flow

A. Control of the Bidirectional Power Flow

As shown in Fig. 4, the dc-bus voltage Udc is always controlled to keep a constant value Uref with zero error by the voltage-feedback control loop. Meanwhile, the direction and magnitude of VS-PWM converter's output current and power are decided dynamically by the value of Ue , which is the output of negative PI regulator in the voltage loop.

If Udc > Uref then Ue is increasing, and the VS-PWM converter works as an inverter which transfers the PV array power to the utility grid. The energy generation of PV power system is positively correlated with the magnitude of Ue .

If Udc < Uref then Ue is decreasing, and when Ue < 0, the VS-PWM converter works as a PWM rectifier, which draws the energy from the utility grid to the capacitor of dc bus, maintaining the stability of dc-bus voltage. The current in the negative direction finally approaches a quite small value, which is only used to compensate for the switch losses of VS-PWM converter.

B. Direct Current Control With Compensation Units

As shown in Fig. 4, the load currents iout is detected and compared with the reference current iref , and the error signal is processed by a PI regulator in the current-feedback control loop. Main advantages of this direct current control are the low harmonics to reduce losses in steady state, the fast response to provide high dynamic performances, and the peak-current protection to reject overload. Generally, the current control loop is designed to have a bandwidth of 2–5 kHz, higher than the voltage loop bandwidth of 200–500 Hz, to assure the stability of the proposed inverter control with two PI regulators.

However, the instantaneous power and the dc-bus voltage include a ripple component with the frequency 2ω in the case of a single phase inverter. Furthermore, the grid voltage is not an ideal sinusoidal waveform in practice. Therefore, it is hard to achieve low THD of the output current by using the simple direct-current-control strategy in the real grid condition. Accordingly, two compensation units are added to the current control loop as the feed forward control units.

The feed forward control has little impact on the system's zeros and poles configuration, but achieves to track the sinusoidal reference accurately and restrain the harmonics distortion of the load current, especially at the current peak.

Compensation coefficient Kd directly processes the magnitude of reference currents iref , and can counteract the main

influences of the dc-bus voltage ripple because Kd represents a negative fluctuating feature with the frequency 2ω, compared with the dc-bus voltage ripple. Kd is defined as

$$K_d = \frac{U_{\text{ref}}}{U_{\text{dc}}}. \tag{4}$$

TABLE II
P&O ALGORITHM EMPLOYING U_e

Perturbation in D	Change in U_e	Next perturbation in D
Positive	Positive	Positive
Positive	Negative	Negative
Negative	Positive	Negative
Negative	Negative	Positive

The PI regulator in the grid-voltage-feed forward control multiplies the real, defective grid voltage with a proportion Kf . Its output uc and the output ua of PI regulator in current feedback loop are together fed to the PWM   modulator to produce the drive signals for the inverter switches. Therefore, the modulation wave uout includes the defective component of grid voltage to compensate grid voltage fluctuation and obtain highly sinusoidal current waveform. The feed forward effect depends on the value of Kf . In addition, the frequency ω and phase φ of current reference iref are calculated to synchronize with utility grid voltage ugrid in real time by a phase-locked-loop (PLL) system, which is achieved via the digital algorithm of DSP chip in this paper

IV. EXPERIMENTAL RESULTS

To confirm the theoretical analysis   in the previous sections, a 2-kW prototype of the proposed grid-connected PV power system was built. Two ZVT-interleaved boost converters of 1 kW are connected in parallel via a dc bus through a central inverter of 2 kW to the grid. The lower power dc-dc converters are connected respectively to the individual PV arrays, and the central inverter can expand the power rate and reduce the system cost. If suppose single block is designed for 50v grid voltage is 500 we need to connect 500/50v = 10 blocks in cascaded connection. If suppose another customer required 1000 v we need to connect 20 blocks in cascade.1000/50. So we need not to re design our system for different grid voltage
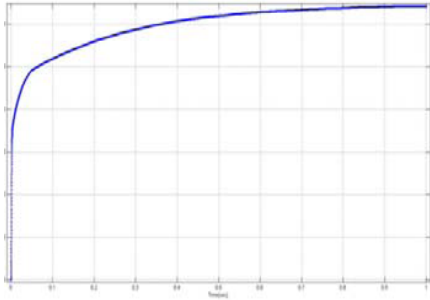
Fig 5 Output Of The Solar Unit

4
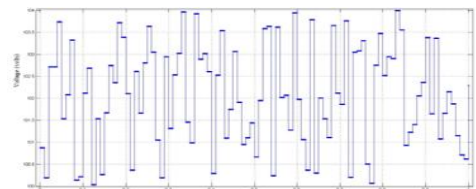
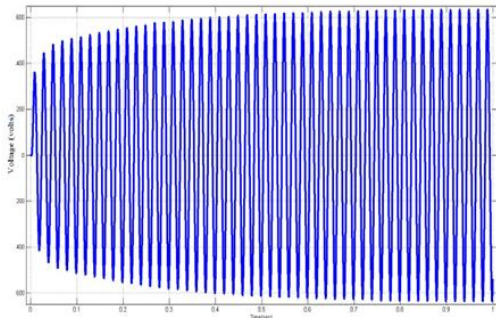**Fig 5 Output Of The Solar Unit**
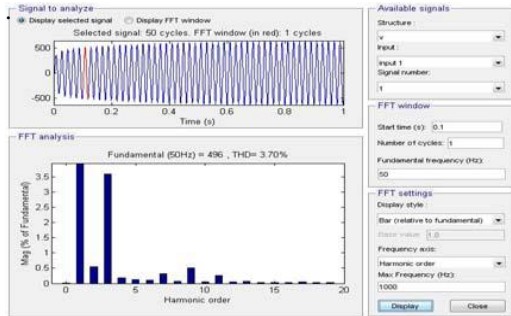

Fig 7. Output Of The cascaded System


Fig 8 FFT Analysis Tool - THD

From the figure 7 by selecting the Harmonic Order we can find the Total Harmonic Distortion (THD). With this proposed system the Total Harmonic Distortion (THD) has been reduced to 3.7%.

It can be clearly seen that the output current is highly sinusoidal synchronized with the grid voltage, which is hardly deteriorated by the ripple component with the frequency 2ω of the dc-bus voltage due to the two compensation units. Fig. 8 shows the harmonic spectrum of the output current at 2 kW, and the measured THD counted till to 50th is 3.384%

Fig. 8. Experimental results about full-bridge inverter with bidirectional power flow. (a) Output current and dc-bus voltage waveforms in the rectify- ing condition. (b) Output current and dc-bus voltage waveforms in the inverting condition.

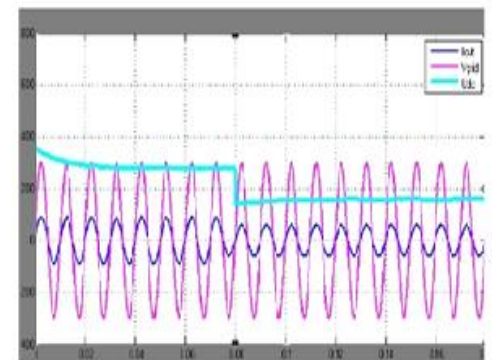Fig. 9. Experimental results of the system dynamic response

under different step source changes. (a) Dynamic response under power source change from 500 to 1600 W. (b) Dynamic response under power source change from 1600 to 500 W.
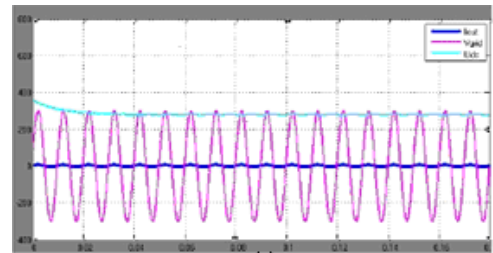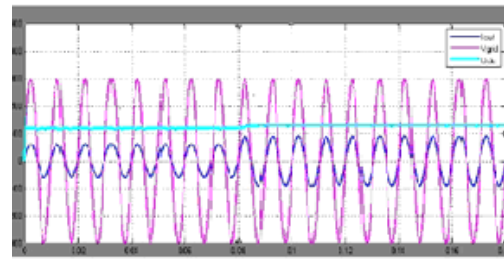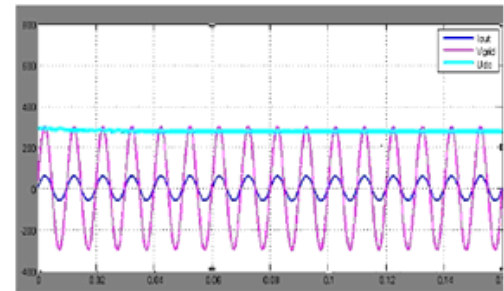
CONCLUSION

This paper presents a grid-connected PV power system with high voltage gain. The proposed PV system employs a high step-up ZVT-interleaved boost converter with winding-coupled inductors and active-clamp circuits as the first power-processing stage, and high voltage gain is obtained by the turns ratio selection of winding-coupled inductors. In conventional system a single PV cell is connected to a dc - dc converter and the output of the dc – dc converter is connected to the inverter finally inverter feeds the

5

power into the grid. In this system inverter and DC - DC converter are rated for grid voltage, so the cost of the whole system is high and reliability is low. Another problem is the inverter output is not a pure AC so we need to use large size filter. The Proposed system eliminates all above disadvantages. In this system DC - DC coverer and inverter are rated for lower voltage and such blocks are connected in cascade to meet the grid voltage. Since we are using low voltage components the overall cost of the system is less and is high. As by using this cascaded inverter, the requirement of high rated filter is reduced which will further reduces cost, complexity of the system and THD.

REFERENCES

REFERENCES

[1] S. B. Kjaer, J. K. Pedersen, and F. Blaabjerg, "A review of single-phase grid-connected inverters for photovoltaic modules," *IEEE Trans. Ind. Appl.*, vol. 41, no. 5, pp. 1292–1306, Sep./Oct. 2005.

[2] Q. Li and P.Wolfs, "A review of the single phase photovoltaic module integrated converter topologies with three different DC link configurations,"
IEEE Trans. Power Electron., vol. 23, no. 3, pp. 1320–1333, May 2008.

[3] M. Calais, J.Myrzik, T. Spooner, and V. G. Agelidis, "Inverters for singlephase grid connected photovoltaic systems—An overview," in *Proc. IEEE PESC*, 2002, vol. 4, pp. 1995–2000.

[4] S. B. Kjær, J. K. Pedersen, and F. Blaabjerg, "Power inverter topologies for photovoltaic modules—A review," in *Proc. IEEE IAS Conf.*, 2002,,pp. 782–788.

[5] Q. Li and P.Wolfs, "A current fed two-inductor boost converter with an integrated magnetic structure and passive lossless snubbers for photovoltaic module integrated converter applications," *IEEE Trans. Power Electron.*, vol. 22, no. 1, pp. 309–321, Jan. 2007.

[6] M. P. Kazmierkowski and L. Malesani, "Current control techniques for three-phase Voltage-Source PWM converters: A survey," *IEEE Trans. Ind. Electron.*, vol. 45, no. 5, pp. 691–703, Oct. 1998.

[7] H. M. Kojabadi, B. Yu, I. A. Gadoura, L. Chang, and M. Ghribi, "A novel DSP-based current-controlled PWM strategy for single phase grid connected inverters," *IEEE Trans. Power Electron.*, vol. 21, no. 4, pp. 985–993, Jul. 2006.

[8] R. Gonzalez, J. Lopez, P. Sanchis, and L. Marroyo, "Transformerless inverter for single-phase photovoltaic systems," *IEEE Trans. Power Electron.*, vol. 22, no. 2, pp. 693–697, Mar. 2007.

[9] T. Kerekes, R. Teodorescu, and U. Borup, "Transformerless photovoltaic inverters connected to the grid," in *Proc. IEEE APEC Conf.*, 2007, pp. 1733–1737.

[10] O. Lopez, R. Teodorescu, F. Freijedo, and J. Doval-Gandoy, "Eliminating ground current in a transformerless photovoltaic applictation," in *Proc. IEEE PES Conf.*, 2007, pp. 1–5.

[11] R. Gonzalez, E. Gubia, J. Lopez, and L.Marroyo, "Transformerless singlephase multilevel-based photovoltaic inverter," *IEEE Trans. Ind. Electron.*, vol. 55, no. 7, pp. 2694–2702, Jul. 2008.

[12] German Patent, "HERIC-topology," Patent DE 10 221 592 A1, Dec. 4, 2003.

[13] German Patent, "H5-topology," Patent DE 102 004 030 912 B3, Jan. 19, 2006.

[14] International Patent, "Circuit arrangement having a twin inductor for converting a DC voltage into an AC voltage or an alternating current," Patent WO/2007/077031, Jul. 12, 2007.

[15] *2005 National Electrical Code*, National Fire Protection Association, Quincy, MA, 2005.

[16] H. Haeberlin, "Photovoltaik." Berlin, Germany: VDE Publishing House, 606 pp. (in German). ISBN: 978-3-8007-3003-2.

[17] W. Li and X. He, "ZVT interleaved boost converters for high-efficiency, high step-up DC/DC conversion," *IET Electr. Power Appl.*, vol. 1, no. 2, pp. 284–290, Mar. 2007. [9] H.Akagi, "New trends in active filters for power conditioning," IEEE Industry Applications., vol. 32, No-6, pp. 1312-1322, 1996

[18] Q. Zhao and F. C. Lee, "High-efficiency, high step-upDC–DC converters," *IEEE Trans. Power Electron.*, vol. 18, no. 1, pp. 65–73, Jan. 2003.

[19] R. J.Wai and R. Y. Duan, "High step-up converter with coupled-inductor," *IEEE Trans. Power Electron.*, vol. 20, no. 5, pp. 1025–1035, Sep. 2005.

[20] K. C. Tseng and T. J. Liang, "Novel high-efficiency step-up converter," *IEE Electr. Power Appl.*, vol. 151, no. 2, pp. 182–190, Mar. 2004.

[21] F. C. Lee, S. Wang, P. Kong, C. Wang, and D. Fu, "Power architecture design with improved system efficiency, EMI and power density," in *Proc. IEEE PESC Conf.*, 2008, pp. 4131–4137.

[22] A. Bellini, S. Bifaretti, and V. Iacovone, "Resonant DC–DC converters for photovoltaic energy generation systems," in *Proc. IEEE SPEEDAM Conf.*, 2008, pp. 815–820.

[23] D. Fu, F. C. Lee, Y. Liu, and M. Xu, "Novel multi-element resonant converters for front-end dc/dc converters," in *Proc. IEEE PESC Conf.*, 2008, pp. 250–256.

[24] D. Fu, F. C. Lee, Y. Qiu, and F. Wang, "A novel high-power-density three level LCC resonant converter with constant-power-factor-control for charging applications," *IEEE Trans. Power Electron.*, vol. 23, no. 5, pp. 2411–2420, Sep. 2008.

[25] M. P. Kazmierkowski and L. Malesani, "Current control techniques for three-phase Voltage-Source PWM Converters: A survey," *IEEE Trans. Ind. Electron.*, vol. 45, no. 5, pp. 691–703, Oct. 1998.

[26] M. Cichowias and M. P. Kamierkowski, "Comparison of current control techniques forPWMrectifiers," in *Proc. IEEE Int. Symp.*, 2002, pp. 1259– 1263.

[27] T. Esram and P. L. Chapman, "Comparison of photovoltaic array maximum

6